Intermediate-depth earthquakes triggered by localized heating in peridotites

The surface plates of Earth (thickness, ~60 km), on which we live, move and subduct along with the flow of the mantle (depths greater than 60 km). Earthquakes occur through the collision and subduction of plates. Earthquakes can be divided into three types according to the depth of hypocenter: i) interplate or crustal earthquakes (depths <50 km); ii) intermediate-depth earthquakes (50–300 km); and iii) deep earthquakes (>300 km). Intermediate-depth earthquakes often occur in subduction zones, and sometimes magnitude 7-class ones result in serious disasters. However, the occurrence of intermediate-depth earthquakes in subducting slabs has long puzzled geoscientists because these earthquakes require some mechanism to accelerate the fault movement at pressures above 1.8 GPa (i.e., depths ≥50 km). The frictional strength is so high that fault movement is inhibited without a "lubricant" at such high pressures. Since 1960s, a generally accepted hypothesis has been that aqueous fluid released from the breakdown reaction of hydrous minerals (e.g., antigorite and lawsonite) triggers intermediate-depth earthquakes. However, the distribution of hydrous minerals, and thus the aqueous fluid, is limited to the upper part of subducting slabs, namely, aqueous fluid does not account for the occurrence of earthquakes in the lower part of slabs. Here we show that intermediate-depth earthquakes could be caused by the drastic weakening of peridotites (i.e., the main constituent of slabs) through localized heating followed by partial melting [1].

My colleagues and I have conducted uniaxial deformation experiments on peridotite samples combined with synchrotron *in situ* X-ray observations at pressures of 1.0–2.6 GPa, temperatures of 860–1350 K and strain rates of 10^{-5}–10^{-4} s^{-1} using a deformation-DIA apparatus at SPring-8 **BL04B1**. The temperature and pressure ranges were equivalent to the conditions in the shallower part of subducting slabs. Acoustic emissions (AEs) were monitored using six piezoceramic lead-zirconate titanate transducers, each attached to the rear side of a second-stage anvil. Our AE monitoring technique (Fig. 1) allowed us to evaluate the three-dimensional location and magnitude of microcracks (i.e., hypocenters of AEs) in a deforming peridotite sample. The mechanical and statistical similarities between AEs and earthquakes have been verified on the basis of the Gutenberg-Richter relationship and the accelerated moment release model. In particular, the dependence of the critical nucleation size of failure on the duration of quasi-dynamic rupture is known to follow a scaling relationship in a wide range of scales from micrometers (i.e., microcracks) to kilometers (i.e., earthquakes) [2].

The plastic deformation of peridotite samples was followed by faulting and AEs at an accelerated strain rate ($>5\times10^{-5}$ s^{-1}). A decrease in the Gutenberg–Richter *b*-value and increases in the AE amplitude and AE rate were usually observed around the timing of faulting, probably due to the subcritical growth of cracks. Strong AE activity was also observed to continue after the faulting (i.e., aftershocks). Gouge layers consisting of ultrafine-grained olivine and orthopyroxene (down to 20 nm) developed along faults. Amorphous films were frequently observed on the grain interfaces (Fig. 2). Taking into account the possibility of localized heating (i.e., adiabatic instability caused by the weakening-feedback mechanism wherein localized deformation caused further heating), the origin of the amorphous phase must be evaluated from the viewpoint of the partial melting of peridotite. In fact, the following theoretical equation (Eq. 1) [3] predicts that localized heating is effective when the strain rate exceeds a threshold value ($>10^{-4}$ s^{-1} in a laboratory scale):

$$\dot{\varepsilon}_c > \frac{h\rho C_p \kappa R T^2}{\sigma H^* L^2} \tag{1}$$

where h is the work hardening coefficient ($= 1$), ρ is the density (~3.4 g/cm^3 at 1.5 GPa), C_p is the specific
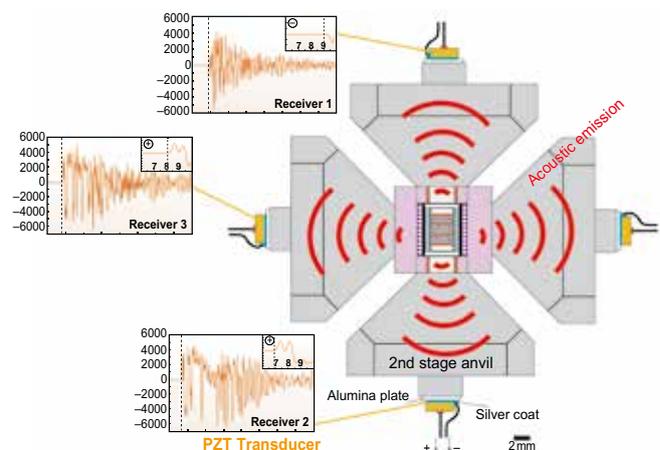
Fig. 1. Cell assembly viewed as a cross section from the direction parallel to the X-ray path. A cylindrical peridotite sample (diameter: 3 mm; length: 5 mm) is placed in the central part of the cell assembly. Piezoceramic lead-zirconate titanate (PZT) transducers are attached to the rear side of second-stage anvils made from tungsten carbide or cubic boron nitride. The transducers are separated from the anvils by alumina plates. Representative waveforms detected by transducers are also shown.
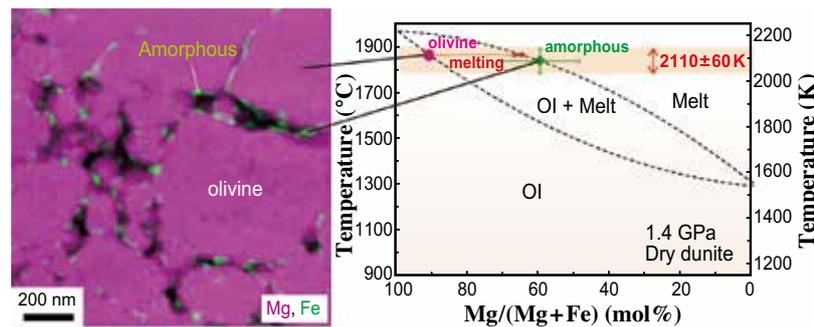
Fig. 2. Element map of ultrafine grains in a gouge layer formed in a failed dunite sample. The map was acquired using a field-emission TEM JEOL-2100F equipped with an EDS detector system at Ehime University. In the element map, the grayscale corresponds to the concentration of elements (pink: magnesium; green: iron). Chemical compositions of olivine and the amorphous phase are plotted in an equilibrium diagram of the $Mg_2SiO_4–Fe_2SiO_4$ system at 1.4 GPa under dry conditions. The iron content of the amorphous phase shows that the melting temperature is 2110±60 K.

heat (= 817 J/kg·K), κ is the thermal diffusivity (= 0.7 mm²/s), H^* is the activation enthalpy for deformation (= 554 kJ/mol at 1.5 GPa), and L is the sample size (= 5.5 mm). *In situ* X-ray observations showed that the fault slip rate observed in the peridotites was sufficient to trigger localized heating. The partitioning of iron between olivine and the melt (i.e., amorphous phase) is useful for estimating the melting temperature in dry dunite (i.e., a monomineralic peridotite that consists of olivine). Using the calibration line determined from the chemical composition of olivine (Mg/(Mg+Fe) = 91 mol%), the concentration of iron in the amorphous phase was determined to be Mg/(Mg+Fe) = 59±11 mol%. The estimated iron content is consistent with the ideal iron content of the partial melt of olivine within the error bar (i.e., Mg/(Mg+Fe) = 65 mol%). Thus, the peak temperature during the localized heating in the dry dunite was estimated to be ~2110±60 K from the iron concentration in the amorphous phase (Fig. 2). At the peak temperature, the creep strength of the faults in dry dunite is thought to decrease to ~35 MPa or less.

Localized heating, which is required for the initiation of faulting, can be achieved in subducting slabs (temperatures of 873–973 K and pressures up to 6.5 GPa). It is obvious that the critical strain rate at a laboratory scale (i.e., ~10⁻⁴ s⁻¹) is much higher than that at a natural scale (1–10 km thickness for each plane of the double seismic zone) (see Eq. 1). Taking into account the fact that the plastic deformation of peridotites follows a power-law form in the shallow upper mantle, localized heating is considered possible once the background strain rate exceeds a threshold value in the range from 10⁻¹⁵ to 10⁻¹³ s⁻¹. The strain rate can be easily increased to the threshold value in shear zones as a result of dynamic recrystallization (i.e., grain size reduction via dislocation creep) followed by diffusion creep (Fig. 3). Localized heating

induced by strain localization in the fine-grained peridotite shear zone has also been verified by a numerical model [4] and geological observations [5]. Thus, we conclude that the formation of fine-grained shear zones may be important for the occurrence of intermediate-depth earthquakes triggered by localized heating in subducting slabs.
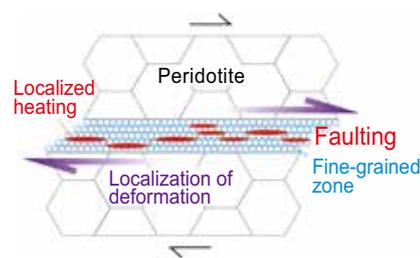
Fig. 3. Schematic diagram showing faulting caused by accelerated strain localization in peridotite with a fine-grained shear zone. The dominant deformation mechanisms are dislocation creep and diffusion creep in the coarse-grained wall rock (gray) and in the fine-grained shear zone (blue), respectively. Accelerated strain localization triggers localized heating in the fine-grained shear zone.

Tomohiro Ohuchi

Geodynamics Research Center, Ehime University

Email: ohuchi@sci.ehime-u.ac.jp

References
[1] T. Ohuchi, X. Lei, H. Ohfuji, Y. Higo, Y. Tange, T. Sakai, K. Fujino and T. Irifune: Nat. Geosci. **10** (2017) 771.
[2] X. Lei et al.: Phys. Earth Planet. Inter. **137** (2003) 213.
[3] S. Karto: An Introduction to the Rheology of Solid Earth (2008) Cambridge Univ. Press.
[4] P.B. Kelemen, G. Hirth: Nature **446** (2007) 787.
[5] T. Ueda et al.: Geology **36** (2008) 607.